Mott Transition and Glassiness in the Face Centered Cubic Lattice

Rajarshi Tiwari and Pinaki Majumdar
Harish-Chandra Research Institute,
Chhatnag Road, Jhusi, Allahabad 211019, India
(Dated: 12 Feb 2013)

We study the half-filled Hubbard model on the geometrically frustrated face centered cubic (FCC) lattice, using an auxiliary field based real space technique. The low temperature state is a paramagnetic metal at weak interaction, an antiferromagnetic insulator (AFI) with flux like order at intermediate interaction, and an AFI with 'C type' order at very strong interaction. Remarkably, there is a narrow window between the paramagnetic metal and the AFI where the system exhibits spin glass behaviour arising from the presence of disordered but 'frozen' local moments. The spin glass state is metallic at weaker interaction but shows crossover to pseudogap behaviour and an insulating resistivity with growing interaction. We compare our results to available experiments on FCC and pyrochlore based materials and suggest that several of these features are typical of three dimensional correlated systems with geometric frustration.

The presence of geometric frustration in an interacting electron system disfavours long range magnetic order and promotes a complex electronic state with short range correlations[1,2]. Such effects have been intensely explored in the context of the quasi two dimensional (2D) organic salts[3,4] where, in some compounds, the triangular lattice structure gives rise to a spin liquid rather than conventional Neel order.

Unlike in 2D, there is no organised body of work probing the interplay of geometric frustration and Mott physics in three dimensions (3D). There are intriguing experimental results on disparate systems[5–25], whose common features do not seem to have been noticed. The 3D frustrated Mott systems are realised on face centered cubic (FCC) and pyrochlore lattices. They both involve corner sharing tetrahedra, disfavouring simple Neel order in the insulating phase. The FCC examples include the cluster compounds[5–8] like $GaTa_4Se_8$, $GaNb_4Se_8$, *etc*, some alkali fulleride's of the form[9–12] A_3C_{60}, and the 'B site ordered' double perovskites[13–17], *e.g.*, Sr_2InReO_6. The pyrochlore examples include the molybdates[18–20] $R_2Mo_2O_7$ and iridates[21–25] $Ln_2Ir_2O_7$. Most of these materials, at ambient 'pressure'[26], are insulators close to a Mott transition.

While there is great variation among these materials, the following features seem to be shared: (a). In the Mott phase they usually exhibit no long range order down to the lowest temperature, sometimes with a hint of 'spin freezing'[5,14,15,17–19]. (b). On pressure driven metallisation, the resistivity is *very large but finite*[7,20,24,25] at low temperature over a wide pressure window, and exhibits a negative temperature derivative, before eventual 'normal' behaviour. (c) Optical conductivity[8,24], where available across the pressure driven transition, indicates large transfer of spectral weight. (d) The Hall conductance[23] has a spontaneous anomalous contribution indicating significant non coplanar character in the magnetic background. In addition, (e). some of these systems exhibit superconductivity at low temperature[7,9–12].

The complexity of the three dimensional structures has prevented a detailed exploration of the possible magnetic phases and the Mott transition in these systems. While each material involves its specific electronic model, in this paper we focus on the single band Hubbard model at half-filling on the FCC lattice. We use an approach that captures the unrestricted Hartee-Fock (UHF) state at zero temperature, but retains the crucial thermal fluctuations of the interaction induced 'local moments', and their impact on electronic properties. Using a combination of Monte Carlo (MC) and variational schemes we establish the following: (*i*) In the ground state, increasing interaction leads, successively, to transition from a

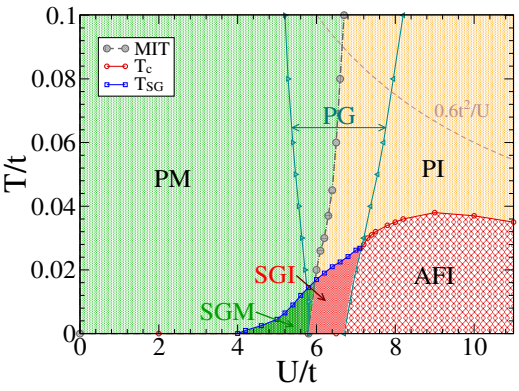

FIG. 1: The $U-T$ phase diagram of the Hubbard model on the FCC lattice at half-filling. The ground state can be a paramagnetic metal (PM), with no local moments, a spin glass metal (SGM) or spin glass insulator (SGI) with disordered local moments, and an antiferromagnetic insulator (AFI). The AFI has 'flux' like order upto $U/t \approx 30$, beyond which it has 'C type' order. The classification into 'metal' and 'insulator' is based on the temperature dependence of the resistivity, $\rho(T)$. $d\rho/dT > 0$ indicates a metal, $d\rho/dT < 0$ an insulator. At finite temperature the system also has a paramagnetic (Mott) insulating (PI) phase. The magnetic transition temperature, T_c, and the spin glass freezing temperature, T_{SG} (see text), are indicated. We show the extrapolation of the $T_c \sim 0.6t^2/U$ asymptote, that describes the $U/t \gg 1$ transition, to highlight the large deviation from the short range Heisenberg result. The PG region involves a pseudogap in the density of states.

paramagnetic metal (PM) to a spin glass metal (SGM), a spin glass 'insulator' (SGI), and then an antiferromagnetic insulator (AFI). The AFI has flux like order at weaker coupling, and 'C type' order (see Supplement) in the very strong coupling Heisenberg limit. (*ii*) The T_c scales in the ordered phase, as well as the notional glass transition temperature T_{SG}, are a tiny fraction, $\sim$ a few percent, of the hopping scale due to the frustration. (*iii*) While the AFI phase has a clear gap and divergent resistivity as temperature $T \to 0$, the spin glass insulator has a pseudogap (PG) in the single particle density of states (DOS), non Drude optical response, and *large but finite resistivity* at $T = 0$ with $d\rho/dT < 0$. (*iv*) The transport trends match remarkably with experiments on FCC Mott systems, and allow us to make predictions about their magnetic and spectral properties.

There is surprisingly little theoretical work on the magnetic phases or the Mott transition in the FCC lattice. There is a very early calculation exploring a restricted set of mean field states[27] but, in contrast to two dimensions, there does not seem to be any cellular dynamical mean field theory (C-DMFT) result handling the combination of correlation and frustration. We use an approach, suggested long back by Hubbard himself[28], for the model:

$$H = \sum_{\langle ij \rangle \sigma} t_{ij} c^\dagger_{i\sigma} c_{j\sigma} - \mu \sum_i n_i + U \sum_i n_{i\uparrow} n_{i\downarrow} \qquad (1)$$

The $t_{ij} = -t$ for nearest neighbour hopping on the FCC lattice. We will set $t = 1$ as the reference energy scale. μ controls the electron density, which we maintain at $n = 1$. $U > 0$ is the Hubbard repulsion.

We use a Hubbard-Stratonovich (HS) transformation[29] that introduces a vector field $\mathbf{m}_i(\tau)$ and a scalar field $\phi_i(\tau)$ at each site to decouple the interaction. This decomposition[28,30] retains the rotation invariance of the Hubbard model and reproduces UHF theory at saddle point. We treat the $\mathbf{m}_i$ and ϕ_i as classical fields, *i.e*, neglect their time dependence, but completely retain the thermal fluctuations in $\mathbf{m}_i$. ϕ_i is treated at the saddle point level, *i.e*, $\phi_i \to \langle \phi_i \rangle = (U/2)\langle\langle n_i \rangle\rangle = U/2$ at half-filling, since charge fluctuations would be penalised at temperatures $T \ll U$. Retaining the spatial fluctuations of $\mathbf{m}_i$ allows us to estimate T_c scales, and access the crucial thermal effects on transport. We will discuss the limitations of the method later in the paper.

With this approximation the half-filled Hubbard problem is mapped on to electrons coupled to field, $\mathbf{m}_i$.

$$H_{eff} = \sum_{ij,\sigma} t_{ij} c^\dagger_{i\sigma} c_{j\sigma} - \tilde{\mu} N - \frac{U}{2} \sum_i \mathbf{m}_i \cdot \vec{\sigma}_i + \frac{U}{4} \sum_i \mathbf{m}_i^2 \quad (2)$$

where $\tilde{m}u = \mu - U/2$. We can write this as $H_{eff} = H_{el}\{\mathbf{m}_i\} + H_{cl}$, where $H_{cl} = (U/4)\sum_i \mathbf{m}_i^2$. The $\{\mathbf{m}_i\}$ configurations follow the distribution $P\{\mathbf{m}_i\} \propto Tr_{c,c^\dagger} e^{-\beta(H_{el}+H_{cl})}$.

Within the static HS approximation H_{eff} and $P\{\mathbf{m}_i\}$ define a coupled fermion-local moment problem. This is similar to the 'double exchange' problem, with the crucial difference that the moments are self generated (and drive the Mott transition) rather than fixed in size. Due to the fermion trace, $P\{\mathbf{m}_i\}$ is not analytically calculable beyond weak coupling. To generate the equilibrium $\{\mathbf{m}_i\}$ we use Monte-Carlo sampling. Computing the energy cost of an attempted update requires diagonalising H_{el}. To access large sizes within limited time, we use a cluster algorithm for estimating the update cost. We calculate the energy cost of an update by diagonalizing a cluster (of size N_c, say) around the reference site. We have extensively benchmarked this 'traveling cluster' method[31]. The static HS approach, retaining spatial fluctuations, has found successful application in correlated systems before[33]. The MC was done for lattices of size upto $N = 12 \times 12 \times 12$, with clusters of size $N_c = 4 \times 4 \times 4$. We calculate the thermally averaged structure factor $S(\mathbf{q}) = \frac{1}{N^2}\sum_{ij}\langle \mathbf{m_i} \cdot \mathbf{m_j} \rangle e^{i\mathbf{q}\cdot(\mathbf{r}_i - \mathbf{r}_j)}$ at each temperature. The onset of rapid growth in $S(\mathbf{q})$ at some $\mathbf{q} = \mathbf{Q}$, say, with lowering T, indicates a magnetic transition. Electronic properties (see Supplement) are calculated by diagonalising H_{el} on the full lattice for equilibrium $\{\mathbf{m}_i\}$ configurations. Since the MC ground state can be affected by annealing protocol, wherever possible we have tested it against variational choices of $\{\mathbf{m}_i\}$.

Fig.1 shows the $U - T$ phase diagram of our model. First focus on the magnetism at $T = 0$. (*i*) The MC based minimization, $\frac{\delta}{\delta \mathbf{m}_i}\langle H_{eff}\{\mathbf{m}_i\}\rangle = 0$, leads to a state with $m_i = |\mathbf{m}_i| = 0$ for $U < U_{c1} \sim 4t$. (*ii*) For $U_{c1} < U < U_{c2}$, where $U_{c2} \sim 6.7t$, the ground state involves finite m_i, with a finite width distribution $P(m, U) = \langle \frac{1}{N}\sum_i \delta(m - |\mathbf{m}_i|)\rangle$, but with no long range spatial correlation. The system behaves like a spin glass with short range 'flux like' correlations. (*iii*) Beyond U_{c2} the ground state has long range flux like order till $U \sim 30t$, beyond which the virtual hopping generated exchange is effectively nearest neighbour and we obtain 'C type' order. The C type order is indeed expected[34] for the AF Heisenberg model on the FCC lattice.

The thermal physics deep in the AFI phase is controlled by angular fluctuations of the local moments, $\mathbf{m}_i$, about the ordered state. For $U \gg U_{c2}$ this leads to the usual $T_c \propto t^2/U$, but with a coefficient of ≈ 0.6, much smaller than ~ 1.4 in the simple cubic case. At weaker interaction, for $U_{c2} < U \lesssim 30t$, longer range and multi-spin couplings between the $\mathbf{m}_i$ become relevant and the T_c deviates significantly from the t^2/U asymptote. For $U \lesssim 9t$ the size of the local moment itself diminishes rapidly, due to increase in itinerancy, and the T_c falls sharply. Below $U_{c2} \sim 6.7t$ where we have a glassy phase we make a crude estimate of the 'freezing temperature' from the MC based local relaxation time[32], $\tau_{av}(T, U) = (1/N)\sum_i \int_0^{t_{max}} dt \langle \mathbf{m}_i(0).\mathbf{m}_i(t)\rangle$. If the system undergoes an ordering transition, on lowering T, there is a rapid growth in τ_{av} accompanied by a growth in the structure factor $S(\mathbf{q})$ at the $\mathbf{q}$'s associated with long range order (LRO). For a glass transition, one observes similar growth in τ_{av}, without any signatures in

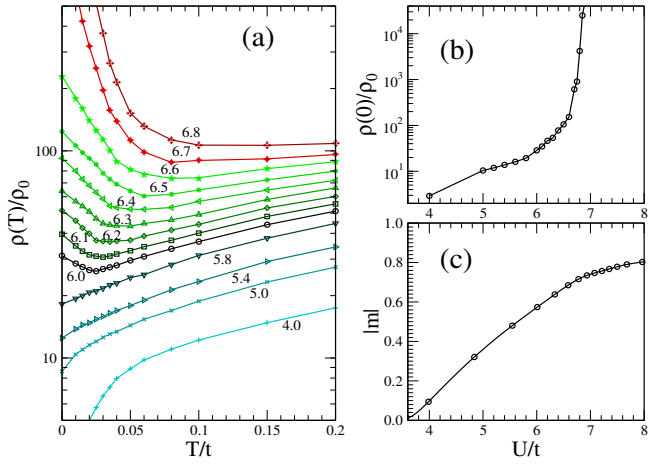

FIG. 2: Colour online: (a) Temperature and U dependence of the resistivity. The U/t values are marked in the plot. In the PM window, $U < U_{c1}$, the zero temperature resistivity $\rho(0)$ vanishes and $d\rho/dT > 0$ at low T. In the SGM phase, $U_{c1} < U < U_c$, $\rho(0)$ is finite, with $d\rho/dT > 0$. In the SGI phase, *i.e*, $U_c < U < U_{c2}$, $\rho(0)$ is finite, rapidly grows with U, and shows $d\rho/dT < 0$. For $U > U_{c2}$ where the ground state has long range order and a gapped spectrum, $\rho(0)$ is infinite, and $d\rho/dT < 0$. For the weakly insulating ground states, $(U - U_c)/U_c \ll 1$, increasing temperature leads to a crossover to $d\rho/dT > 0$ beyond a temperature we call $T_{IMT}(U)$. (b) The variation of the $\rho(0)$ with U/t. (c) The variation of the average moment m_{av} at $T = 0$ with U. Our resistivity is measured on the scale of $\rho_0 \sim \hbar a_0/\pi e^2$, where a_0 is the lattice spacing. For $a_0 \sim 3\mathring{A}$ it will be $\sim 60\mu\Omega$cm.

$S(\mathbf{q})$. For $U > U_{c2}$ we observe LRO as well as a rapid increase in τ_{av} at a single temperature $T_c(U)$. For the window $U_{c1} < U < U_{c2}$, however, τ_{av} rises, at a temperature we call $T_{SG}(U)$, *without associated LRO*. We have also 'heated' the system up from $T = 0$ and discovered that any assumed ordered state is quickly destabilized while the moments themselves survive. T_{SG} varies in the manner shown in Fig.1, vanishing for $U < U_{c1}$ where there are no local moments.

Fig.2 shows the resistivity $\rho(T, U)$. For $U < U_{c1}$ the resistivity $\rho(T = 0) = 0$, and $d\rho/dT > 0$. For $U > U_{c2}$ the system is gapped at $T = 0$, $\rho(T = 0) \to \infty$ and $d\rho/dT < 0$. These are the obvious metallic and insulating behaviour that one expects across a correlation driven transition. For $U_{c1} < U < U_{c2}$, however, the $T = 0$ resistivity is *finite*, with $d\rho/dT > 0$ for $U_{c1} < U < U_c$, where $U_c \approx 5.8t$, and $d\rho/dT < 0$ for $U_c < U < U_{c2}$. This behaviour would usually not be expected in a translation invariant system, and arises because of the scattering of electrons from the 'frozen' local moments. The growth of $m_{av}(U)$, the mean magnitude of m_i, leads to the enhanced scattering with increasing U and finally the divergence of $\rho(0)$ due to the opening of a gap. The variation of $\rho(0)$ and m_{av} with U/t are shown in panels (b) and (c) respectively. We characterize the system as metallic, at a given T and U, when $d\rho/dT > 0$, and insulating when $d\rho/dT < 0$. With this convention, an 'insulator' may have finite spectral weight at $\omega = 0$ in the optical conductivity $\sigma(\omega)$.

While the $U > U_{c2}$ system would have a gapped DOS, and the $U < U_{c1}$ case is likely to have a featureless DOS, the glassy window in between may have unusual spectral features. Fig.3.(a)-(b) shows the DOS for varying U/t at $T = 0.03t$ and $T = 0.20t$, respectively. For lack of space the colour codes for U/t are marked in panel (b) only. In panel (a), for $U \lesssim U_{c1}$ the DOS is featureless, but for $5.4 < U/t < 7.5$ it displays a PG, and for higher U/t there is a clear gap. The large U/t phase is magnetically ordered at this temperature. At the higher temperature in panel (b), where there is no trace of magnetic order, the PG feature extends over a much larger U/t window. The weaker U 'metals' in (b) have a deeper PG compared to panel (a), while the weak gap insulators now have a PG feature rather than a hard gap. The evolution in panel (b) essentially illustrates the paramagnetic Mott transition on the FCC lattice.

Panels 3.(c)-(e) show the T dependence of the DOS for three typical U/t in the glassy window, where the ground state has frozen local moments. They all share the feature of thermally induced loss of low frequency

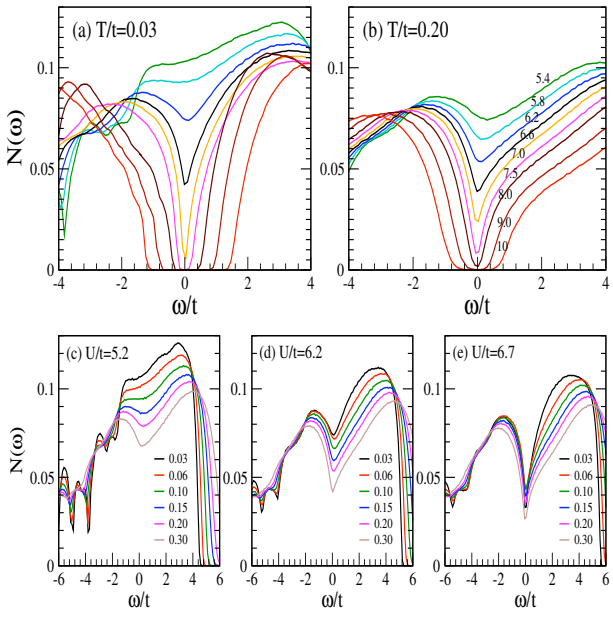

FIG. 3: Colour online: Density of states $N(\omega)$. Panel (a) shows the DOS at $T = 0.03t$ for increasing U/t showing the crossover from a correlated metal to an AFI (with weak surviving order) through a wide pseudogap window. The colour code for U/t is marked in panel (b). Panel (b) shows the DOS at $T = 0.20t$ where the crossover is between the PM and a PI through a much wider pseudogap window. Panels (c)-(e) show the temperature dependence at three fixed U in the spin glass window. Notice the emergence of a thermally induced PG at weak interaction, $U = 5.2t$, and the presence of the PG at $T = 0$ itself for $U = 6.2t$ and $6.7t$. Modest changes of temperature, $T \sim 0.1t$, leads to large asymmetric shift of spectral weight from $\omega \sim 0$ to $\omega \sim U$.

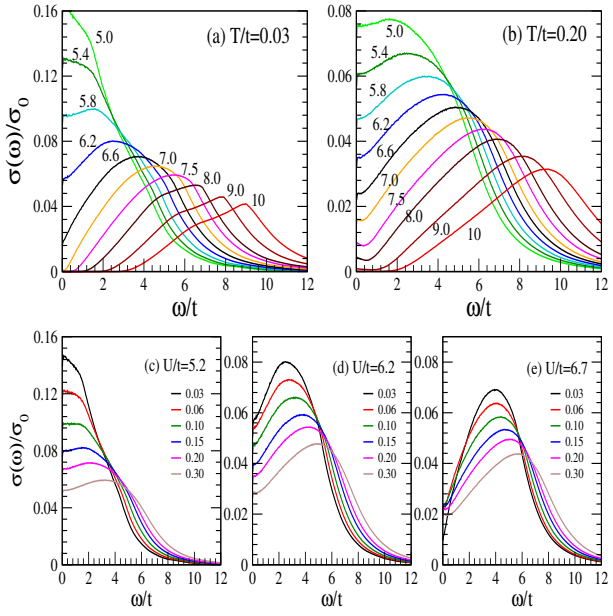

FIG. 4: Colour online: Optical conductivity $\sigma(\omega)$. Panel (a) shows $\sigma(\omega)$ at $T = 0.03t$ for increasing U/t (marked in the plot). The response evolves from a Drude character to the gapped spectrum of the AFI through a non Drude regime. Panel (b) shows similar evolution at $T = 0.20t$, from the PM to a PI. There is no Drude peak visible down to $U = 5t$, the peak locations have moved to higher ω, and the overall scale of $\sigma(\omega)$ is halved. Panels (c)-(e) show the temperature dependence of $\sigma(\omega)$ for some U/t in the spin glass window. The weak moment system in (c) shows essentially a broadening Drude response with increasing T. The larger moment system with $U/t = 6.2$ in (d) shows a non Drude response with low frequency weight suppressed by temperature for $T > 0.03t$. Panel (e) shows a spin glass with large $T = 0$ resistivity. The very low frequency weight (on the scale of the pseudogap) *increases with* T, while the weight at $\omega \sim U$ reduces with increasing T. The scale $\sigma_0 = 1/\rho_0$.

weight which shows up at $\omega \sim U$. There is markedly less change with T on the negative frequency side, particularly in panels (d) and (e), compared to positive frequencies. This is due to the large asymmetry in the tight binding DOS of the FCC lattice. There is a subtle low energy difference between panels (c)-(d) and panel (e). In (c)-(d) the loss in low frequency weight, within $\omega \sim \pm t$ is monotonic with T. In panel (e), however, which neighbours the AFI, the low frequency weight first *increases* with T, upto $T \sim 0.1t$, and then again diminishes at higher temperature.

Fig.4 shows the optics for the same parameter choice as the DOS plots. Panels (a)-(b) show the evolution of $\sigma(\omega)$ across the metal-insulator transition, between the PM and AFI at $T = 0.03t$, and between the PM and PI at $T = 0.20t$. There is a clear window of non Drude response at low T, roughly corresponding to the PG regime in Fig.3.(a). In 4.(b) the non Drude window in U/t has increased as in Fig.3.(b) with a general suppression in the magnitude of $\sigma(\omega)$. The panels (c)-(e) show the suppression of low frequency optical weight, with some of it appearing at $\omega \gtrsim U$. Unlike the single particle DOS, the total optical weight is not conserved and varies with the kinetic energy. At $U/t = 6.7$, the very low frequency optical response is non monotonic in T, showing a quick increase and then a gradual suppression. This directly relates to the behaviour of $\rho(T)$ in Fig.2.(a).

We have highlighted a host of magnetic, transport and spectral features associated with Mott phenomena on the FCC lattice. However, like all many body methods, our approach too is approximate and let us touch upon the possible shortcomings before we attempt to relate our results to experiments. Earlier papers[28,30] have set out the formalism so we do not enter into it again here.

The ground state that we access through MC is equivalent to the UHF result, but *with no assumptions about translational symmetry.* It is easy to see some of the qualitative effects of dynamical fluctuations in $\mathbf{m}_i$ and ϕ_i, that we have neglected, at $T = 0$. These would (i) convert the $U < U_{c1}$ PM to a correlated metal, (ii) introduce quantum spin fluctuations in the large U AFI, and (iii) possibly shift U_{c1} to a larger value (since the correlated metal competes better with the local moment phase). The intermediate window 'spin glass' that appears within the static approximation might be converted to a spin liquid with slowly fluctuating moments. A recent calculation on the triangular lattice demonstrates how longer range and multi-spin interactions arise on a frustrated Mott insulator and can lead to a spin liquid ground state[35].

Our approach captures the correct thermal fluctuations of the $\mathbf{m}_i$, without any assumption about LRO in the background. This in turn allows us to capture a T_c that has the qualitatively correct U dependence. With growing temperature, but staying at $T \ll U$, these classical thermal fluctuations should reasonably describe the magnetic background, and its effect on the electrons.

While our solution of the FCC Mott problem involves approximation, and real materials usually require interactions and degrees of freedom beyond the Hubbard description, our results suggest the organization of a broad class of experiments. (i) We find that a non coplanar spin configuration dominates the Mott phase, and pressure induced metallisation leads to a weak moment 'spin frozen' state with short range non coplanar correlations. This is consistent[6,9,12] with observations on $GaTa_4Se_8$, FCC A_3C_{60}, and double perovskite materials. (ii) Beyond the pressure driven IMT the materials exhibit[7,20,22,24] very high $\rho(0)$, and $d\rho/dT < 0$. Our results show how this can arise from the presence of disordered local moments strongly coupled to the itinerant electrons, leading to large scattering. In the Ga cluster materials these local moments emerge from correlation effects, while in the pyrochlores[20] they are already present as localised a_{1g} electrons. (iii) The very recent optical measurement[8] in $GaTa_4Se_8$ shows pronounced non Drude character in the metal near the IMT. This is consistent with our optics results for the PM to PI transition. In fact we have a

quantitative description of the Mott transition in these materials[36] within our present framework.

The correspondence above allows us to make two concrete predictions: (a) The frustrated Mott systems should have a wide pseudogap regime beyond the insulator-metal transition, persisting to $T = 0$. These should be visible in tunneling and photo-emission spectra. (b). The thermally induced shift of single particle spectral weight would be *extremely asymmetric*. Weight at low positive frequencies is shifted to the scale of $\omega \sim U$, while the negative frequency spectrum remains almost unaffected.

We have not probed the anomalous Hall response due to flux like correlations and plan to present them separately. Some of the FCC Mott materials have a superconducting instability at very low temperature, $\sim$ 10K. We have not treated that aspect, and need a method that retains the dynamics of the $\mathbf{m}_i$ to do so.

Conclusions: We have provided the first comprehensive study of the Mott transition on the geometrically frustrated FCC lattice. The magnetic frustration leads to a seemingly 'two fluid' state of itinerant electrons and disordered local moments between the paramagnetic metal and the antiferromagnetic insulator. The disordered phase involves a large residual resistivity, non Drude optical response, and a single particle pseudogap. The temperature and interaction dependence that we uncover allows a common conceptual scheme for a wide variety of materials.

We acknowledge use of the HPC clusters at HRI. PM acknowledges support from a DAE-SRC Outstanding Research Investigator grant.

[1] N. P. Ong and R. J. Cava, Science, **305**, 52 (2005).
[2] L. Balents, Nature, **464**, 199 (2010).
[3] B. J. Powell and R. H. McKenzie, Rep. Prog. Phys. **74**, 056501 (2011).
[4] K. Kanoda, J. Phys. Soc. Jpn. **75**, 051007 (2006).
[5] R. Pocha, *et al.*, J. Am. Chem. Soc. **127**, 8732 (2005).
[6] S. Jakob, *et al.*, J. Mat. Chem. **17**, 3833 (2007).
[7] M. M. Abd-Elmeguid, *et al.*, Phys. Rev. Lett. **93**, 126403 (2004).
[8] V. Ta Phuoc, *et al.*, Phys. Rev. Lett. **110**, 037401 (2013).
[9] T. Takenobu, T. Muro, Y. Iwasa, and T. Mitani, Phys. Rev. Lett. **85**, 381 (2000).
[10] Massimo Capone, Michele Fabrizio, Claudio Castellani, Erio Tosatti, Rev. Mod. Phys. **81**, 943 (2009).
[11] Alexey *et al*, Nature **466**, 221 (2010).
[12] Y. Ihara, H. Alloul, P. Wzietek, D. Pontiroli, M. Mazzani, and M. Ricco, Phys. Rev. Lett. **104**, 256402 (2010).
[13] C. R. Wiebe, J. E. Greedan, G. M. Luke, and J. S. Gardner, Phys. Rev. B **65**, 144413 (2002).
[14] T. Aharen, *et al.*, Phys. Rev. B **80**, 134423 (2009).
[15] T. Aharen, *et al.*, Phys. Rev. B **81**, 064436 (2010).
[16] M. A. de Vries, A. C. Mclaughlin, and J.-W. G. Bos, Phys. Rev. Lett. **104**, 177202 (2010).
[17] H. Gao, *et al.*, Phys. Rev. B **83**, 134406 (2011).
[18] B. D. Gaulin, J. N. Reimers, T. E. Mason, J. E. Greedan, and Z. Tun, Phys. Rev. Lett. **69**, 3244 (1992).
[19] M. J. P. Gingras, C. V. Stager, N. P. Raju, B. D. Gaulin, and J. E. Greedan, Phys. Rev. Lett. **78**, 947 (1997).
[20] S. Iguchi, N. Hanasaki, M. Kinuhara, N. Takeshita, C. Terakura, Y. Taguchi, H. Takagi, and Y. Tokura, Phys. Rev. Lett. **102**, 136407 (2009).
[21] S. Nakatsuji, *et al.*, Phys. Rev. Lett. **96**, 087204 (2006).
[22] K. Matsuhira, *et al.*, J. Phys. Soc. J. **76**, 043706 (2007).
[23] Y. Machida, S. Nakatsuji, Y. Maeno, T. Tayama, T. Sakakibara, and S. Onoda, Phys. Rev. Lett. **98**, 057203 (2007).
[24] K. Ueda, J. Fujioka, Y. Takahashi, T. Suzuki, S. Ishiwata, Y. Taguchi, and Y. Tokura, Phys. Rev. Lett. **109**, 136402 (2012).
[25] F. F. Tafti, J. J. Ishikawa, A. McCollam, S. Nakatsuji, and S. R. Julian, Phys. Rev. B **85**, 205104 (2012).
[26] The effective 'pressure' can also be of chemical origin, driven by change in ionic radius.
[27] D. Grensing, E. Marsch, and W. H. Steeb, Phys. Rev. B **17**, 2221 (1978).
[28] J. Hubbard, Phys. Rev. B **19**, 2626 (1979).
[29] R. L. Stratonovich, Sov. Phys. Doklady **2**, 416 (1958), J. Hubbard, Phys. Rev. Lett. **3**, 77 (1959).
[30] H. J. Schulz, Phys. Rev. Lett. **65**, 2462 (1990).
[31] S. Kumar and P. Majumdar, Eur. Phys. J. B, **50**, 571 (2006).
[32] K. Binder and A. P. Young, Rev. Mod. Phys. **58**, 801 (1986).
[33] Y. Dubi, Y. Meir and Y. Avishai, Nature, **449**, 876 (2007).
[34] M. V. Gvozdikova and M. E. Zhitomirsky, JETP Lett., **81**, 236 (2005).
[35] H. Y. Yang, A. M. Lauchli, F. Mila and K. P. Schmidt, Phys. Rev. Lett. **105**, 267204 (2010).
[36] R. Tiwari and P. Majumdar, unpublished.

Supplementary information:

A. Magnetic phases on FCC lattice

In the cubic lattice notation, the primitive lattice translation vectors for FCC are $\mathbf{A_1} = a(0,1,1)$,$\mathbf{A_2} = a(1,0,1)$,$\mathbf{A_3} = a(1,1,0)$, so that the nearest neighbour distance is $d_{fcc} = \sqrt{2}a$. All the points on FCC lattice are expressed in integer units of these, i.e., $X = \sum_{i=1}^{3} n_i A_i = a(n_2+n_3, n_3+n_1, n_1+n_2)$. Each site has 12 neighbours $X+\delta$, where δ=$(\pm1,\pm1,0),(\pm1,0,\pm1),(0,\pm1,\pm1)$. The 'flux' phase mentioned in the text, is described by the following formula

$$\mathbf{m}(X) = m(e^{iQ_1\cdot X}, e^{iQ_2\cdot X}, e^{iQ_3\cdot X})/\sqrt{3}$$

Where, m is magnitude of the vector, and $Q_1 = (\frac{\pi}{a},0,0)$, $Q_2 = (0,\frac{\pi}{a},0)$, $Q_3 = (0,0,\frac{\pi}{a})$. Its a non-coplanner phase. On the other hand, the 'C-type' phase is a collinear one, described by the formula

$$\mathbf{m}(X) = m(0,0,e^{iQ_c\cdot X})$$

Where, $Q_c = (\frac{\pi}{a},\frac{\pi}{a},0)$. It consists of alternating ferromagnetic lines. Both the 'flux' and 'C-type' phases are shown in Fig.5 in the top and bottom panel respectively.

B. Derivation of the effective Hamiltonian

Consider the single band Hubbard model as starting point

$$\begin{aligned} H &= \sum_{\langle ij\rangle\sigma} t_{ij} c^\dagger_{i\sigma} c_{j\sigma} - \mu \sum_i n_i + U \sum_i n_{i\uparrow} n_{i\downarrow} \\ &= H_0 - \mu \sum_i n_i + U \sum_i n_{i\uparrow} n_{i\downarrow} \end{aligned}$$

and implement a rotation invariant decoupling of the Hubbard term as follows. First, we write

$$n_{i\uparrow} n_{i\downarrow} = \frac{n_i^2}{4} - (\vec{s}_i \cdot \hat{\mathbf{m}}_i)^2$$

where $n_i = n_{i\uparrow} + n_{i\downarrow}$ is the charge density, $\vec{s}_i = \frac{1}{2}\sum_{\alpha,\beta} c^\dagger_{i\alpha} \vec{\sigma}_{\alpha\beta} c_{i\beta} = 2\vec{\sigma}_i$ is the local electron spin operator, and $\hat{\mathbf{m}}_i$ is an *arbitrary unit vector*.

The partition function of the Hubbard model is

$$\begin{aligned} Z &= \int D[c,\bar{c}] e^{-S} \\ S &= \int_0^\beta d\tau \mathcal{L}(\tau) \\ \mathcal{L} &= \sum_{i\sigma} \bar{c}_{i\sigma}(\tau)\partial_\tau c_{i\sigma}(\tau) + H(\tau) \end{aligned}$$

We introduce two space-time varying auxiliary fields for a Hubbard-Stratonovich transformation: (i) $\phi_i(\tau)$ coupling to charge density, and (ii) $\Delta_i(\tau)\hat{\mathbf{m}}_i(\tau) = \mathbf{m}_i(\tau)$ coupling

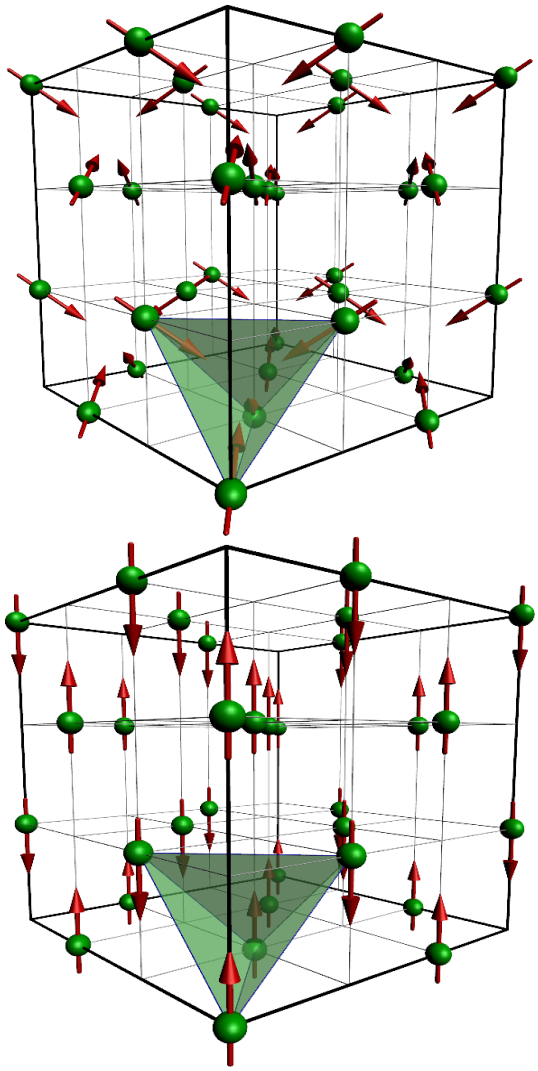

FIG. 5: Color online: The 'flux' (top) and 'C-type' (bottom) phases, drawn on cubic lattice motif. The green spheres are the FCC lattice points, and arrows indicate the direction of $\mathbf{m_i}$ moments. The tetrahedra highlights the geometrical frustration.

to electron spin density (Δ_i is real positive). This allows us to define an SU(2) invariant HS transformation[1,2],

$$e^{U n_{i\uparrow} n_{i\downarrow}} = \int \frac{d\phi_i d\mathbf{m}_i}{4\pi^2 U} e^{\left(\frac{\phi_i^2}{U} + i\phi_i n_i + \frac{\mathbf{m_i^2}}{U} - 2\mathbf{m}_i\cdot\vec{s}_i\right)}$$

The partition function now becomes:

$$\begin{aligned} Z &= \int \prod_i \frac{d\bar{c}_i dc_i d\phi_i d\mathbf{m}_i}{4\pi^2 U} e^{\left(-\int_0^\beta \mathcal{L}(\tau)\right)} \\ \mathcal{L}(\tau) &= \sum_{i\sigma} \bar{c}_{i\sigma}(\tau)\partial_\tau c_{i\sigma}(\tau) + H_0(\tau) + \mathcal{L}_{int}(\phi_i(\tau), \mathbf{m}_i(\tau)) \\ \mathcal{L}_{int} &= \sum_i \left[\frac{\phi_i^2}{U} + i\phi_i n_i + \frac{\mathbf{m}_i^2}{U} - 2\mathbf{m}_i\cdot\vec{s}_i\right] \end{aligned}$$

As mentioned in the text, to make progress we use two approximations: (i) neglect the time (τ) dependence of

the HS fields, (ii) replace the field ϕ_i by its saddle point value $(U/2)\langle n_i\rangle = U/2$, since the important low energy fluctuations arise from the $\mathbf{m}_i$. Simplifying the action with above substitution, we get the effective Hamiltonian

$$H_{eff} = H_0 - \tilde{\mu}\sum_i n_i - \sum_i \mathbf{m}_i\cdot\vec{\sigma}_i + \sum_i \frac{\mathbf{m}_i^2}{U}$$

where $\tilde{\mu} = \mu - U/2$. For the sake of convenience we rescale $\mathbf{m}_i \to \frac{U}{2}\mathbf{m}_i$, so that the $\mathbf{m}_i$ is dimensionless. This leads to the effective Hamiltonian that we used in the text:

$$H_{eff} = H_0 - \tilde{\mu}\sum_i n_i - \frac{U}{2}\sum_i \mathbf{m}_i\cdot\vec{\sigma}_i + \frac{U}{4}\sum_i \mathbf{m}_i^2$$

The partition function can be written in terms of H_{eff}

$$Z = \int \mathcal{D}\mathbf{m}_i Tr_{c,c^\dagger} e^{-\beta H_{eff}}$$

For a given configuration $\{\mathbf{m}_i\}$ the problem is quadratic in the fermions, while the configurations themselves are obtained by a MC sampling as discussed in the text.

C. Optical conductivity

The conductivity of is calculated as follows (ref.[3]), using the Kubo formula:

$$\begin{aligned}\sigma^{xx}(\omega) &= \frac{A}{N}\sum_{\alpha,\beta}\frac{n_\alpha - n_\beta}{\epsilon_\beta - \epsilon_\alpha}|\langle\alpha|J_x|\beta\rangle|^2\delta(\omega - (\epsilon_\beta - \epsilon_\alpha))\\ J_x &= -it\sum_{i,\sigma}\left[(c^\dagger_{i,\sigma}c_{i+\hat{x}+\hat{y},\sigma} - \text{hc})\right]\end{aligned}$$

Where, J_x is the current operator and, the coefficient $A = \frac{\sigma_0}{2a} = \frac{\sigma_0}{\sqrt{2}d_{fcc}}$. $\sigma_0 = \frac{\pi e^2}{\hbar}$ is the scale for conductivity with dimension of conductance.

$n_\alpha = f(\epsilon_\alpha)$ is the Fermi function, and ϵ_α and $|\alpha\rangle$ are respectively the single particle eigenvalues and eigenstates of H_{eff} in a given background $\{\mathbf{m}_i\}$. N is the number of sites ($N = 12^3$ in our results). The results we show in the text are averaged over equilibrium MC configurations.

The d.c conductivity is the $\omega \to 0$ limit of the result above. The experimental value of d_{fcc} for the $GaTa_4Se8$ cluster compound is $\sim 4.3\mathring{A}$.

[1] Weng, Z. Y. and Ting, C. S. and Lee, T. K., Phys. Rev. B **43** 3790 (1991)

[2] K. Borejsza and N. Dupuis, Europhys. Lett. **63** 722 (2003)

[3] P. B. Allen in *Conceptual Foundation of Materials V.2*, edited by Steven G. Louie, Marvin L. Cohen, Elsevier (2006).